Journal of Magnetic Resonance **139,** 46–59 (1999)
Article ID jmre.1999.1759, available online at http://www.idealibrary.com on IDEAL®

The Accuracy of Distance Measurements in Solid-State NMR

Paul Hodgkinson[1] and Lyndon Emsley[2]

Laboratoire de Stéréochimie et des Interactions Moléculaires (CNRS/ENS-Lyon), Ecole Normale Supérieure de Lyon, 46 allée d'Italie, 69364 Lyon, France

Received October 16, 1998; revised March 3, 1999

The accuracy with which distances can be measured using dipolar recoupling experiments in solid-state NMR is investigated. The relative precision of experiments in a three spin system versus an isolated spin pair is found to depend very strongly on the nature of the coupling Hamiltonian. The accuracy of distances measured in even the simplified three spin system is seen to be very poor for existing homonuclear recoupling Hamiltonians. This suggests that it would be difficult to exploit broadband *homonuclear* recoupling to measure geometrical information reliably in complex spin systems. These conclusions apply equally to both single-crystal studies and powder samples. In contrast, the presence of additional spins has marginal impact on the accuracy when the coupling Hamiltonians commute with each other, as in the case of *heteronuclear* recoupling. The possibility of creating such a Hamiltonian for *homonuclear* recoupling using a suitable rotor-synchronized pulse sequence is discussed. © 1999 Academic Press

INTRODUCTION

The measurement of internuclear distances via the dipolar interaction is fundamental to the application of solid-state NMR to molecular structure determination. The suppression of the dipolar interactions by magic angle spinning (MAS), which is needed if sites are to be resolved by their chemical shift, means that the residual couplings are too small for efficient magnetization exchange and thus for accurate measurement of the coupling. Hence, the dipolar coupling must be reintroduced (*1*) if the homonuclear dipolar interaction is to be used to obtain structural information. This is usually done either by selective recoupling, e.g., rotational resonance (*2, 3*) where the rotor frequency is matched to the chemical shift difference, or by a broadband recoupling pulse sequence (*4, 5, 6, 7*) combined with selective labeling to specify the spin pair of interest. Sequential spin-pair selective experiments are, however, time-consuming, not to say expensive if selective labeling is required. Hence the majority of recoupling pulse sequences have been specifically designed to be broadband, that is, insensitive to variations in chemical shift offset, in order to recouple systems of more than two spins simultaneously. To date, however, the complexity of the spin dynamics in such coupled systems appears to have limited the applications of broadband recoupling in multispin systems (*8, 9*). In this paper, we provide a quantitative description of this problem by considering the accuracy of the distances measured in such systems. We examine whether this difficulty is fundamental to multispin systems, and to what extent it is dependent on the nature of the coupling Hamiltonian.

THE ACCURACY OF DISTANCE MEASUREMENTS

We assume a basic exchange type experiment, as shown in Fig. 1, where sites are labeled during t_1 (usually by their chemical shifts), allowed to mix under a dipolar coupling Hamiltonian, and observed during t_2. The results of these experiments are a series of "exchange curves" for each pair of spins.

For simplicity we assume a single observation per rotor cycle, in which case the evolution can be described in terms of a single (average) Hamiltonian during the mixing time. We assume that this Hamiltonian has the form

$$H = \sum_{i<j}^{N} d_{ij} H_{ij}, \qquad [1]$$

where H_{ij} is the (recoupled) dipolar Hamiltonian and d_{ij} is the dipolar coupling between spins i and j,

$$d_{ij} = \frac{\mu_0 \hbar \gamma^2}{2\pi r_{ij}^3}, \qquad [2]$$

where r_{ij} is the internuclear distance. For example, in the RF-driven spin diffusion experiment (*10*) using simple CW spin locking, H_{ij} is a scaled version of the normal high-field homonuclear dipolar coupling Hamiltonian,

$$H_{ij} = P_2(\cos\,\theta_{ij})(2I_{iz}I_{jz} - I_{ix}I_{jx} - I_{iy}I_{jy}), \qquad [3]$$

where θ_{ij} is the angle between the i, j internuclear vector and the magnetic field. We include the $P_2(\cos\,\theta)$ factor in the Hamiltonian rather than the dipolar coupling since the orien-

[1] Current address: Department of Chemistry, University of Durham, South Road, Durham DH1 3LE, United Kingdom.

[2] To whom correspondence should be addressed. E-mail: emsley@ens-lyon.fr.

1090-7807/99 $30.00
Copyright © 1999 by Academic Press
All rights of reproduction in any form reserved.

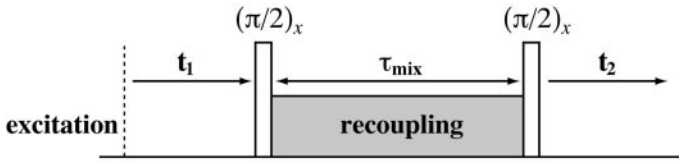

FIG. 1. Pulse sequences for the experiments considered. After excitation of single-quantum coherence (usually by cross-polarization from ^{1}H), the spins are labeled during t_1 and undergo polarization exchange during τ_{mix}. A final $\pi/2$ pulse converts the magnetization into observable single quantum coherence, which is detected during t_2. The mixing periods involve either direct exchange of longitudinal magnetization, e.g., simple "spin-diffusion," radio-frequency driven recoupling (*4, 9*), or the creation of multiple-quantum magnetization followed by reconversion to observable magnetization, e.g., using the C7 sequence (*7, 25*).

tational dependence often varies from one recoupling Hamiltonian to another. Note that chemical shift terms are assumed to have been suppressed during the mixing time in order to maximize coherence transfer via the dipolar coupling.

Once we can calculate the exchange curves for a given spin system and set of dipolar coupling constants, the accuracy with which the dipolar couplings and derived geometrical values can be measured can be determined straightforwardly by calculating the Cramér–Rao lower bounds (CRLBs) on the parameters of interest. These Cramér–Rao lower bounds (or minimum variance bounds) are equal to the standard deviation on the values of parameters measured by model fitting (*11, 12*). An alternative way to calculate these same error bounds is from Monte Carlo simulation of the experiment (*13*), that is, repeatedly fitting a synthesized data set using different noise values and measuring the standard deviation on the resulting distribution of parameter values. Such Monte Carlo simulations are, however, extremely inefficient in comparison with the direct calculation and are only required in situations where the signal-to-noise level is very poor.

The Cramér–Rao lower bounds are calculated via the Hessian matrix, **F**, which has elements

$$F_{ij} = \frac{1}{\sigma^2} \sum_{n}^{K} \mathrm{Re}\left\{ \left(\frac{\partial \hat{y}_n}{\partial \phi_i} \right)^* \frac{\partial \hat{y}_n}{\partial \phi_j} \right\} \qquad [4]$$

where $\hat{y}_n$ is the value of the model function at data point n (out of K) and σ is the rms noise level. The model function is described in terms of the set of parameters ϕ_i.

The standard deviations, $s(\phi_i)$, and correlations, $\mathrm{cor}(\phi_i, \phi_j)$, between the parameters are obtained from the covariance matrix $\boldsymbol{V}$, which is simply the inverse of $\boldsymbol{F}$:

$$s(\phi_i) = \sqrt{V_{ii}} \quad \text{and} \quad \mathrm{cor}(\phi_i, \phi_j) = \frac{V_{ij}}{\sqrt{V_{ii} V_{jj}}}. \qquad [5]$$

Note that, by definition, the error bounds will scale linearly with the signal-to-noise level, σ/α, where α is the overall signal amplitude.

For the experiments being considered, the model function is a function of the distances r_{ij} (or the dipolar couplings, d_{ij}), the inter-bond angles θ_{ij}, a phenomenological relaxation time constant, T_2, and the signal amplitude, α. If the dipolar couplings are strong, then the oscillatory magnetization exchange can be fitted to the coupling/geometrical parameters without significant correlation with the remaining parameters. This allows $\boldsymbol{F}$ to be restricted to r_{ij} and θ_{ij}. For weaker couplings, the relaxation parameters (i.e., T_2) must be included in the calculation of $\boldsymbol{F}$. It is important to note the correlation with α can also be important in this limit. For example, if we observe only the build-up of double quantum coherence between the coupled spins, then the overall signal amplitude is very poorly determined in the limit where relaxation is significant. Hence, the correlations between α, T_2 and the coupling terms become important, resulting in increased error bounds. If, however, we observe the *decay* of longitudinal magnetization or zero-quantum coherence, then the signal amplitude is very well determined from the initial points of the exchange curve. Hence, the correlation with α has negligible impact on the coupling/geometric error bounds. So for experiments involving the recoupling of double-quantum coherence, we select for zero-quantum coherence during the mixing period rather than observing the build-up of the double-quantum coherence.

It is important to emphasize that the numerical values of the calculated bounds are only applicable to experimentally measured values if the systematic errors in fitting the experimental data are significantly smaller than the effects of random errors. Moreover, the number of experimental variables means that it is not realistic to attempt to calculate the precision with which a particular distance can be measured using a particular pulse sequence. This study is concerned solely with the effect of the system Hamiltonian on distance measurement, and the numerical values presented below should not be taken as definitive. The errors for a particular experimental measurement should be calculated from the covariance matrix returned from the fitting procedure.

TWO-SPIN SYSTEMS

For the purposes of structure determination, we are most interested in measuring distances between structural units whose relative position might otherwise be quite poorly defined, e.g., between carbons in distant residues of a protein. Figure 2 shows a histogram of a selected subset of the carbon–carbon distances in the protein BPTI. Four sets of distinct carbon sites have been selected; the backbone carbonyls, the C_α, C_β and methyl carbons. The histogram is calculated from the distances between pairs of carbons *in distinct residues*, which, since they have distinct chemical shift ranges, could in principle be resolved in the 2D exchange spectrum. Clearly the interesting distances are those of at least 4 Å. The experimental

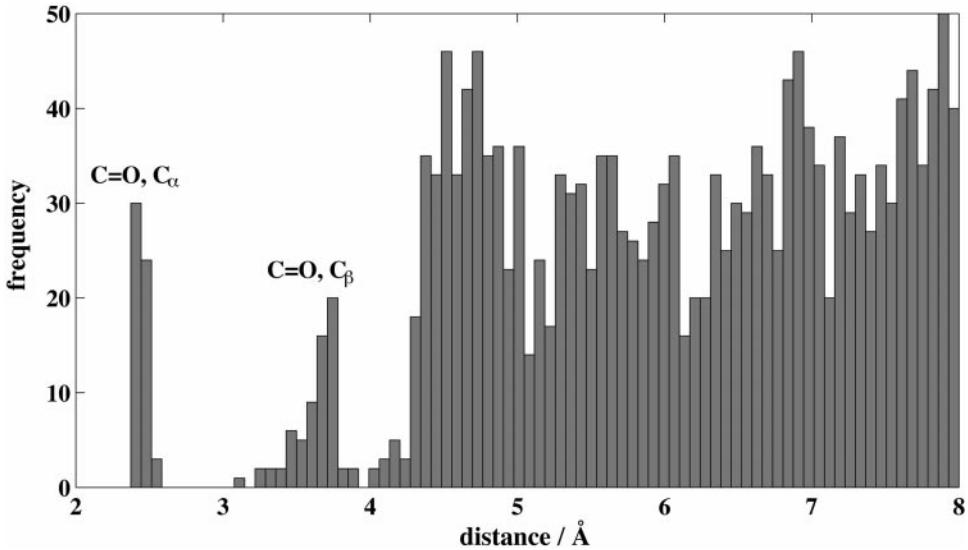

FIG. 2. Histogram of distances between carbons belonging to the sets of (peptide) carbonyls, C_α, C_β, and methyl groups on different peptide residues of BPTI. The resolved peaks in the distribution are readily assigned to the distance between the carbonyl on one residue and the C_α and C_β on the adjacent peptide residue. The rest of the distribution starting at around 4 Å consists of the longer range distances that are critical for structure determination. The crystallographic structural data were taken from Ref. (*14*).

protocol therefore needs to be chosen carefully since these C–C dipolar couplings are less than 120 Hz, before the scaling of the coupling by the recoupling sequence.

Figure 3 plots the standard deviation of the measurement of the dipolar coupling as a function of internuclear separation for an idealized spin-diffusion experiment with the Hamiltonian of Eqs. [1]–[3]. The model function consists of the exchange curve $1 \rightarrow 2$ as well as the diagonal peaks, i.e., 1, 1 and 2, 2. The exchange curve $2 \rightarrow 1$ is identical to the $1 \rightarrow 2$ curve and contains no new information and so is not calculated (although it would be included in a fitting). The precision of the measurement is necessarily a function of the sampling of the data. For simplicity and generality we choose a conventional linear sampling, starting at zero and finishing at a maximum mixing

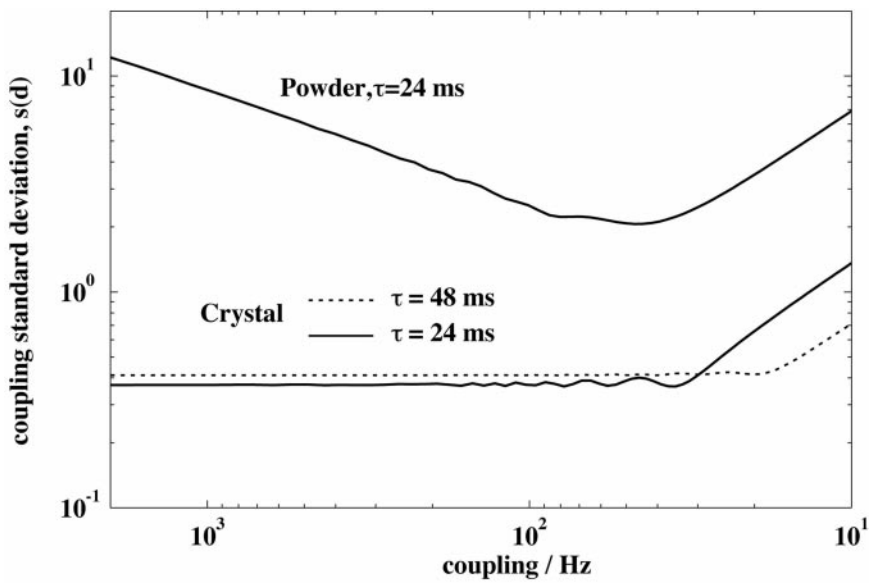

FIG. 3. Standard deviation of the coupling, $s(d)$, between two isolated spins as a function of internuclear distance, using a simulated ideal spin-diffusion experiment, $T_2^{ZQ} = 8$ ms, $\alpha/\sigma = 25$. The lower curves are for a single orientation truncated at $\tau = 48$ ms, $\tau = 24$ ms, and the internuclear vector parallel to the magnetic field. For the powder curve (top), the θ angle was integrated over 350 steps. The points for the largest couplings are extrapolated since a very large number of crystallite orientations are required when the powder linewidth is very much larger than the fundamental linewidth.

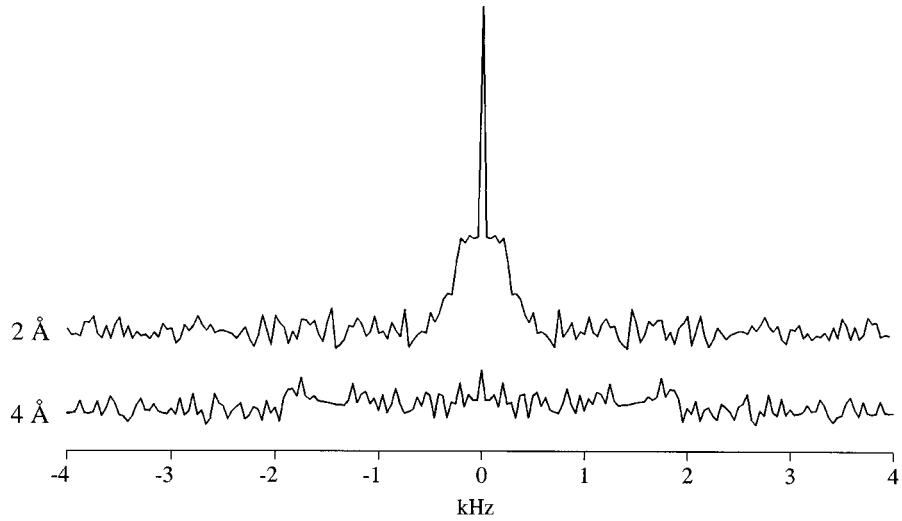

FIG. 4. Fourier transforms of spin-diffusion exchange curves between two spins in a powder sample with noise added (equivalent to $\alpha/\sigma = 40$) using C–C separations of 4 Å ($d = 120$ Hz) and 2 Å ($d = 950$ Hz). The coupling constant can be determined more accurately from the top curve.

time, τ. Note that the number of data points used in the calculations, K, is typically much larger than would be used in experimental practice, to ensure that the oscillation is properly sampled. If the sampling is sufficiently dense, the standard deviations simply scale with $1/\sqrt{K}$ (*15*). The values of bounds have been "normalized" to $K = 32$ points throughout.

For experiments on single crystals—lower traces of Fig. 3—the standard deviation of the coupling is independent of its value for moderate values of the coupling. As the coupling becomes smaller than the linewidth, the standard deviation rises rapidly, $s(d) \propto 1/d$. The critical value of the coupling at which the gradient changes scales with T_2, but also depends to some extent on the truncation of the signal. For poorly resolved couplings, the standard deviation can be markedly reduced by extending the sampling out to long mixing times (e.g., $6T_2$). The fitting of very poorly resolved couplings is, however, very sensitive to systematic errors. Rather than try to attempt to optimize the sampling for each experiment, we use $\tau = 3T_2$ throughout.

The top curve of Fig. 3 shows the result of repeating the calculation for a powder sample, that is, the signal is integrated over the angle θ between the field and the internuclear vector. Since the coupling varies with orientation, the signals from different crystallites interfere, resulting in a damping of the oscillations and, if the signal were to be Fourier transformed, a characteristic broad lineshape. This has a dramatic effect on the accuracy with which the dipolar coupling can be measured; at best the accuracy (as quantified by the standard deviation of the dipolar coupling) is almost an order of magnitude smaller than that for a single orientation (with the same total signal). Counterintuitively at first sight, the accuracy improves as the coupling becomes smaller, until the fundamental limit imposed by the relaxation linewidth is reached. This can be simply explained, however, by the reduction in the width of the powder pattern as the coupling decreases. As the coupling increases, the line becomes so broad that it disappears into the noise, as illustrated in Fig. 4. Within the linewidth limit, the behavior follows that of the single crystal, while maintaining the intrinsic loss in accuracy caused by the orientational variation of the coupling.

For two-spin systems, the standard deviation of the distance measurements can be derived straightforwardly from the coupling results. If we assume a general power law dependence for the coupling as a function of distance, $d = kr^{-n}$, then the error on the distance, $s(r)$, is simply

$$s(r) = \frac{s(d)nr^{(n+1)}}{k} = rs(d)/nd. \qquad [6]$$

We can then define the "reliability" of the distance measurement, $r(r)$, in dimensionless units as the reciprocal of its standard error:

$$r(r) = \frac{r}{s(r)} = nd/s(d). \qquad [7]$$

That is, a reliability of 10 implies that the error on the measurement of r is an order of magnitude smaller than r.

If the log–log plot of $s(d)$ as a function of d has a slope of g, then the plot of $r(r)$ as a function of r will have a slope of $n(g - 1)$. This is confirmed in Fig. 5, where the slopes for the single orientation curve are -3 and -6 for the resolved and unresolved limits, respectively. For the powder sample, $r(r) \propto r^{-1.4}$ in the resolved limit, i.e., the reliability of the distance measurement falls fairly slowly (albeit from a much lower base) as the distance increases. These limiting dependencies are essentially independent of the form of the Hamiltonian,

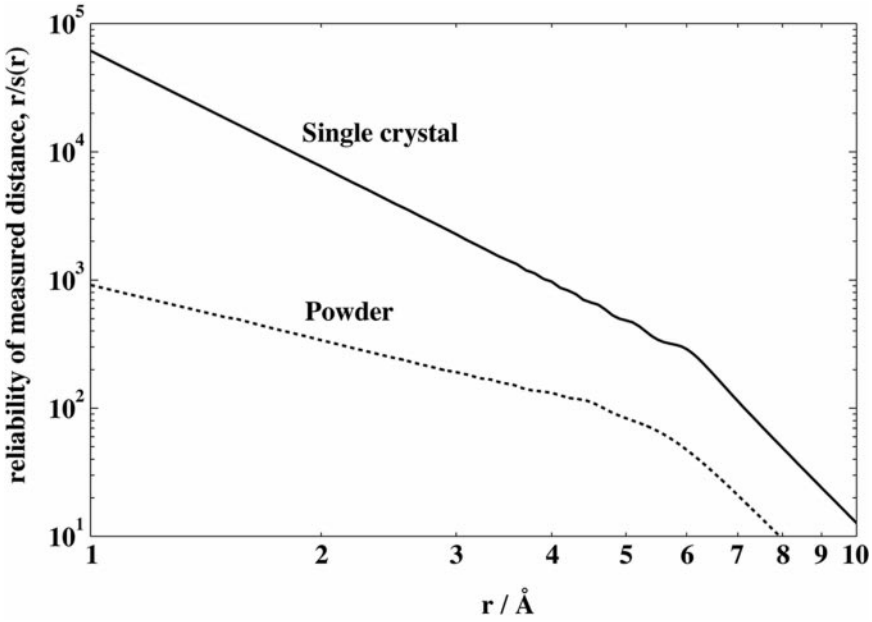

FIG. 5. Reliability of distance measurement for the two spin system of Fig. 3, using $\tau = 24$ ms.

although the behavior at the "transition" from resolved to nonresolved couplings does depend on the Hamiltonian. On the basis of Eq. [7], the accuracy of distance determination will be optimized by choosing the Hamiltonian that recouples most strongly, not least because this maximizes the range of distances over which the couplings are resolved.

We are now in a position to evaluate the effect of changing the nature of the coupling. For instance, we could make use of second-order effects to introduce the dipolar coupling with an r^{-6} dependence (*16, 17*). These "isotropic dipolar shifts" are independent of orientation to first order. At some point, r_0, the reliabilities of the distances obtained using the new interaction and the classic dipolar interaction will be equal. For $r > r_0$, the coupling, d, will fall off very quickly with distance, as will the reliability of r, cf. Eq. [7]. Given the technical difficulties associated with measuring such effects, it would seem that $n > 3$ interactions (including nuclear Overhauser effects) are unlikely to be useful for *quantitative* long-range distance measurements in solid-state NMR.

THREE-SPIN SYSTEMS

Our real interest lies with multispin systems, and the two-spin system considered above serves only as benchmark against which to compare the results for more complex systems. We assume an idealized experiment in which the spins of interest are sufficiently well isolated from the surrounding spins that the signals can be reliably simulated in terms of an isolated multispin system weakly coupled to its environment by relaxation. Although resolved oscillations characteristic of isolated spin systems are routinely observed for spin pairs selected by isotopic labeling or selective recoupling, it is not yet clear whether the time evolution in multisite exchange can be fitted reliably (*8, 9*). For the purpose of this paper, however, we are interested in the proof of principle and we assume that the fitting of such systems is possible without significant distortions introduced by systematic errors. If it can be demonstrated that distance determination in multispin systems is intrinsically unreliable, even for this idealized situation, then there is little virtue in increasing the sophistication of the model.

For our model three-spin system, we choose two carbon nuclei to be separated by a typical C–C bond distance (1.52 Å), with the third, whose position is to be determined, variable. In particular we are interested in determining to what extent the presence of the strong C–C coupling between the notionally bonded carbons affects the precision of the determination of the position of the third nucleus. The position of the "probe" nucleus is measured in polar coordinates with respect to one of the fixed spins. This is a natural choice of geometrical parameters, since the reliability of the measured r value can then be compared directly to the $r(r)$ for the corresponding distance in the two-spin system.

We therefore reduce the number of free parameters to a single linewidth parameter, and the polar coordinates, r and θ, of the third nucleus (see Fig. 6). The distance (or coupling) between the fixed nuclei is not included as a parameter. Since this coupling will be correlated with the other parameters, this amounts to assuming that the strong coupling is known with relatively high precision. Such an assumption is reasonable when we are measuring longer distances. Note that in a mul-

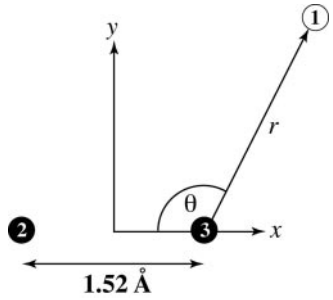

FIG. 6. Coordinates for three-spin systems.

tispin system of general geometry, the simple relationship between coupling standard deviation and distance reliability expressed by Eq. [7] breaks down. Hence, we only consider the fitting of build-up curves directly to geometrical parameters.

The calculation of the evolution in the three-spin system is considerably more involved than that in the two-spin system. Not only has the Hilbert space doubled in size, but the reduction in symmetry means that the powder averaging needs to be performed over the two spherical angles that describe the transformation from the molecular to the laboratory frame, Ω_{MR}. For the simulation of the three-spin system to be efficient, it is necessary to take advantage as far as possible of any block diagonal structure of the Hamiltonian. The spin-diffusion Hamiltonian divides into blocks of constant magnetic quantum number (that is, two 1×1 $I = \pm\frac{3}{2}$ blocks and two 3×3 $I = \pm\frac{1}{2}$ blocks), while the evolution under a double-quantum recoupling Hamiltonian can be separated into two 4×4 blocks ($I = -\frac{1}{2}, \frac{3}{2}$ and $I = -\frac{3}{2}, \frac{1}{2}$). In both cases the evolution in blocks with the same $|I|$ is identical, allowing the spin diffusion evolution, for example, to be calculated using a single 3×3 matrix.

Single-Crystal Results

We first consider the simple case of a single crystal orientation. Since the results will vary with orientation, we show only traces through the full two-dimensional plots of parameter reliability versus the x and y coordinates of the probe spin for one particular orientation. Figure 7 shows the results of the reliability calculation as a function of x with $y = 3$Å. The complex structure of the plots clearly reflects the complex nature of the exchange dynamics in the multispin systems. The lower diagram shows the reliabilities relative to the two-spin system, that is, relative to the reliability of the measurement of the same distance in a two-spin system. The accuracy of the results from the three-spin system is generally many orders of magnitude lower, with the exception of a few special geome-

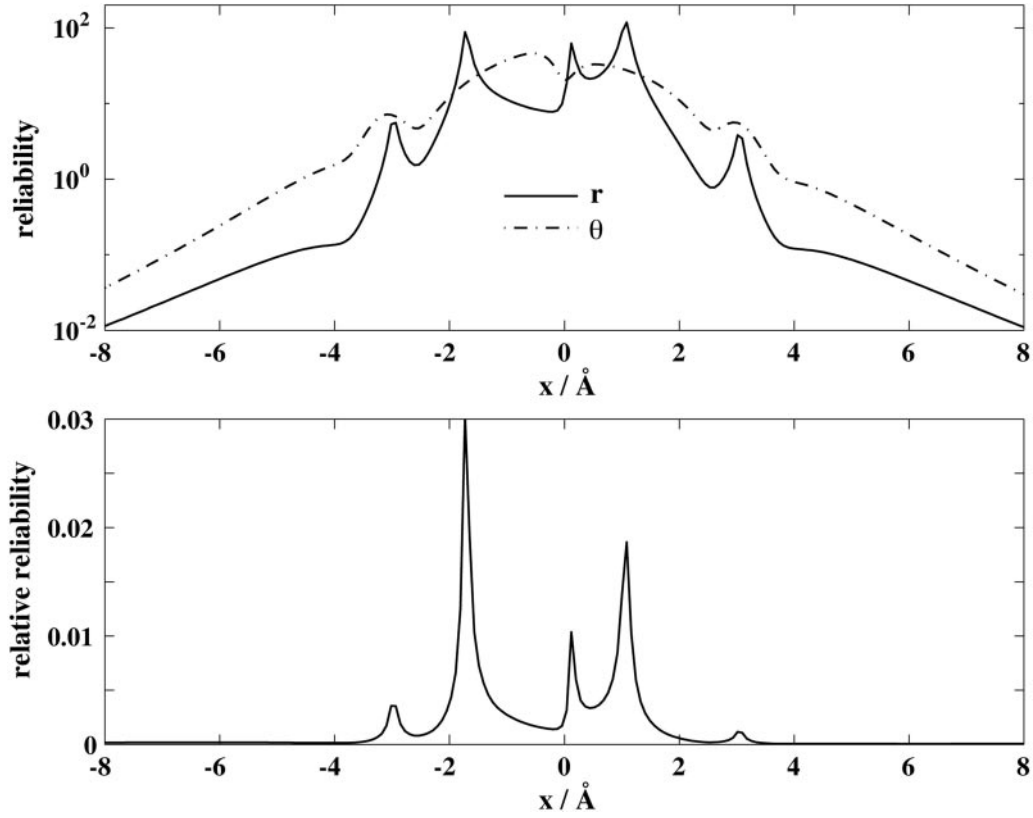

FIG. 7. Reliability calculation for spin diffusion in a three-spin system for a single crystal orientation, $\Omega_{MR} = (0, 0, 0)$. The upper plot shows the reliabilities of r and θ, $r(\theta) = 2\pi/s(\theta)$, as a function of x for $y = 3$Å. The lower plot shows the reliability of r divided by its value in the corresponding two-spin system.

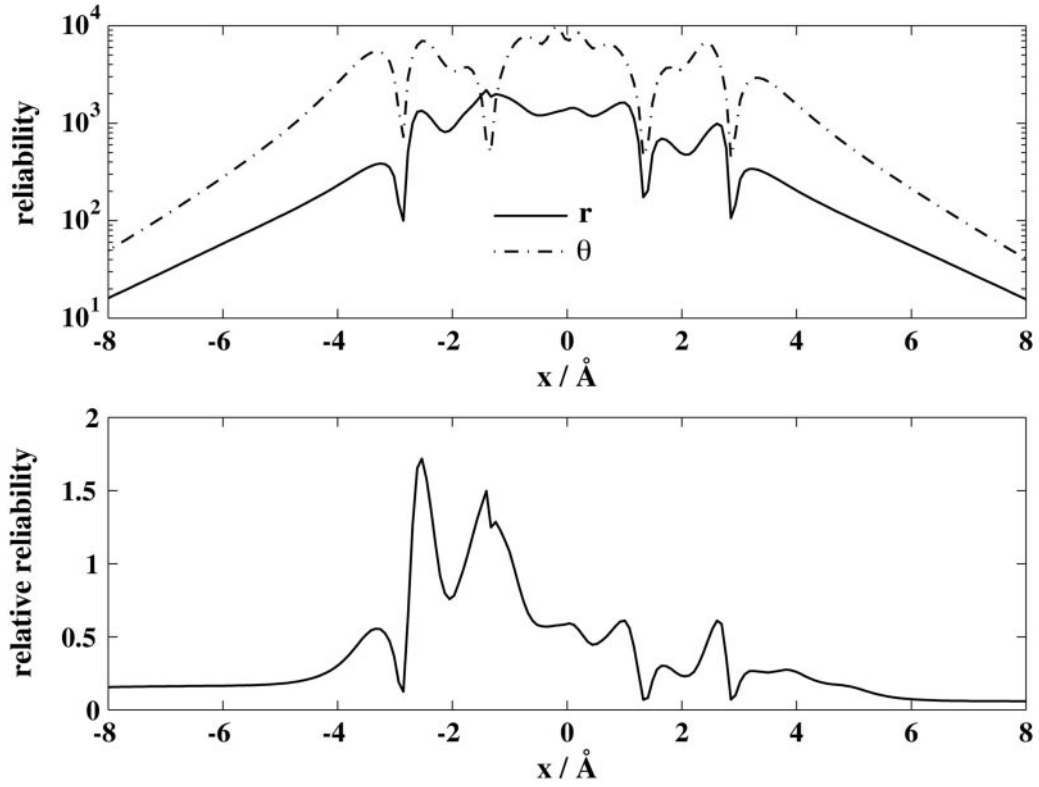

FIG. 8. Reliabilities of the geometrical parameters in a three-spin system for a single crystal orientation, $\Omega_{MR} = (0, 0, 0)$, using the "weak coupling" Hamiltonian of Eq. [8]. The upper plot shows the reliabilities of r and θ, as a function of x for $y = 3$Å. The lower plot shows the reliabilities of r divided by its value in the corresponding two-spin system.

tries. Broadly similar results are observed for other recoupling Hamiltonians, such as the C7 average Hamiltonian.

At this point it would appear that attempts to derive distance information from multispin exchange curves are doomed to failure, or at least unacceptably large errors (or unacceptably long acquisition times). The complexity of the evolution under the spin-diffusion Hamiltonian for three spins is not, however, fundamental to multispin systems, but is largely a consequence of the failure of the individual pair coupling terms to commute among themselves. This is also true of the various existing homonuclear recoupling Hamiltonians. If the pairwise interaction terms did mutually commute, then the evolution would be significantly simpler. The evolution propagator could then be factored into components arising from each pairwise coupling. The spectra would then be given by simple convolutions of the spectra for individual spin pairs, allowing the coupling constants to be determined with relative ease. The much reduced accuracy of parameter fitting in the multispin systems coupled by "homogeneous" Hamiltonians in part reflects the impossibility of separating the evolution into contributions from individual pairwise interactions.

For instance, we consider a "weak coupling" average Hamiltonian

$$H = \sum_{i<j} 2d_{ij}I_{ix}I_{jx}. \qquad [8]$$

This Hamiltonian has the same form as the Hamiltonian for *heteronuclear* recoupling using, for example, REDOR-based pulse sequences (*18, 19*), and assuming that the homonuclear coupling can be neglected or removed. It is also relevant to systems in which the dipolar couplings are so strongly scaled by weakly anisotropic motion that they may be "weak" in comparison with chemical shift differences (*20*). Here we have chosen an "xx" form for the Hamiltonian rather than the "zz" form so that it can be compared more directly with the experiments involving exchange of longitudinal magnetization considered up to this point. Unfortunately, as discussed in the appendix, it appears rather unlikely that such a Hamiltonian can be generated for homonuclear recoupling. There is a good chance that an experiment making use of such a Hamiltonian would be significantly more accurate for measuring longer distances in multispin systems, since the effects of different couplings (large and small) are completely independent. It is noteworthy that REDOR has already been applied to systems of multiple spins (*21, 22*).

Figure 8 shows the reliabilities calculated for the "weak coupling" Hamiltonian in the model three-spin system. Al-

though attempting to compare error bounds between very different experiments is fraught with difficulties, it is clear that the accuracy has been improved dramatically, to the point where the reliabilities in the two- and three-spin systems are fairly similar. Although the three-spin reliability is generally significantly lower than the corresponding two-spin reliability, it can exceed the two-spin value; the added information in the different cross-peak build-up curves ($1 \rightarrow 2$, $1 \rightarrow 3$, $2 \rightarrow 3$) may result in the fitting to a three-spin system being less ambiguous than the corresponding fit in the two-spin system, especially when the two-spin coupling is poorly resolved. There are a few special geometries for which the fitting is very inaccurate. These points change with the orientation of the crystal, and since in practice it would be necessary to perform experiments with a number of different orientations in order to "assign" the signals, they do not pose a significant problem. Note how the relative reliability settles to a constant value in the "unresolved" limit at longer distances. This is also true for the spin diffusion Hamiltonian, Fig. 7, except that this ratio is very much smaller (of the order of 10^{-4}).

This suggests that, with suitable recoupling Hamiltonians, distances could be measured with high precision from single crystals of compounds with nontrivial spin systems. As a rule, however, structures of compounds that crystallize well are determined by X-ray or neutron diffraction. Diffraction-based techniques are unable, however, to distinguish between spatial disorder and temporal disorder caused by molecular motion. For such systems, NMR studies of single crystals, combined with results from diffraction experiments, are a potentially rich source of information about dynamics in the solid phase (*23*).

Powder Samples

Single-crystal studies remain something of a special case, and for the most part, solid-state NMR studies involve powder samples. Hence, we need to calculate the reliabilities that arise after integrating the signal over the isotropic distribution of crystallite orientations. This orientation dependence of the coupling constants inevitably results in broad frequency domain lineshapes. As we have seen for the two-spin system, the accuracy is strongly limited by the relative difficulty of fitting the powder patterns, whatever the form of the Hamiltonian. As a result, we might expect that the relative advantage of the weak coupling Hamiltonian could be reduced.

As has been observed previously, the calculation of derivatives of the model function with respect to the various parameters in the reliability calculation makes it extremely sensitive to the quality of the powder averaging (*24*). As a result, it is necessary to use a rather large number of crystallite orientations. Here we used 120 α orientations and 200 β orientations distributed over a half-sphere. Fortunately powder averaging can be straightforwardly implemented in a parallel fashion, and the calculations were run on a Sun Ultra Enterprise 10000 with the powder loop being divided into small "chunks" distributed as required among up to 8 processors. Even so, with a model data set consisting of 6 exchange curves of 64 points, integrated over 24,000 powder orientations, each data point required about 5 minutes.

Figure 9a shows the result of the reliability calculation for the spin diffusion Hamiltonian in a powder sample, as a function of the position of the probe spin. As expected, the difference between the precision of the two- and three-spin experiments is much smaller for the powder sample than for the single crystal orientation considered earlier. The relative reliability is largest close to the spins, especially when the probe spin is close to the other fixed nucleus. That is to say, the strong perturbing effect of a third spin actually improves the accuracy of the distance determination, since the observed signal is strongly dependent on position when all three spins are close. This effect is very local, however, and for the long distances of interest ($>$4Å), the reliabilities are typically less than 10 or even 1% of their two-spin values, with the exception of some narrow ridges of relatively high accuracy. Unfortunately, the reliabilities calculated from the powder-averaged signal cannot be simply analyzed in terms of contributions from individual orientations. Hence, the detailed structure of Fig. 9 cannot be rationalized directly in terms of special geometries, as was true for the single-crystal results.

The corresponding contour plot for the weak coupling Hamiltonian, Fig. 9b, is very different. There is considerably less variation in the relative reliability, which never drops significantly below unity. *In other words, the precision of the three-spin experiment is about the same as that of the two-spin experiment.* Although the comparison of the precision of two quite different experiments usually involves too many assumptions to be quantitatively useful, it is clear in this case that the precision of the distances measured using a "weak coupling" Hamiltonian in a multispin system are one or even two orders of magnitude better than those recovered from a spin-diffusion-like Hamiltonian.

To illustrate one of the major reasons for this difference, Fig. 10 shows the evolution in time of the three diagonal peaks for two different coupling Hamiltonians. In the case of the spin diffusion Hamiltonian, the strong coupling between the two bonded spins has effectively quenched exchange with the remote third spin. It is clearly impossible to determine the coupling (and the distance) between nonbonded spin pairs. By definition, the strong coupling between the bonded spins cannot interfere with the evolution because of the weaker couplings under a Hamiltonian where the coupling terms mutually commute. Hence, for the weak coupling Hamiltonian, Fig. 10b, the polarization of the remote spin exchanges with the bonded spins. Clearly under these circumstances it is possible to fit the coupling (and the distance) of the remote spin.

This effect can be quantified in terms of the amplitudes of the various frequencies present in the time evolution. The time-domain signal in the eigenbasis of the system Hamiltonian is given by

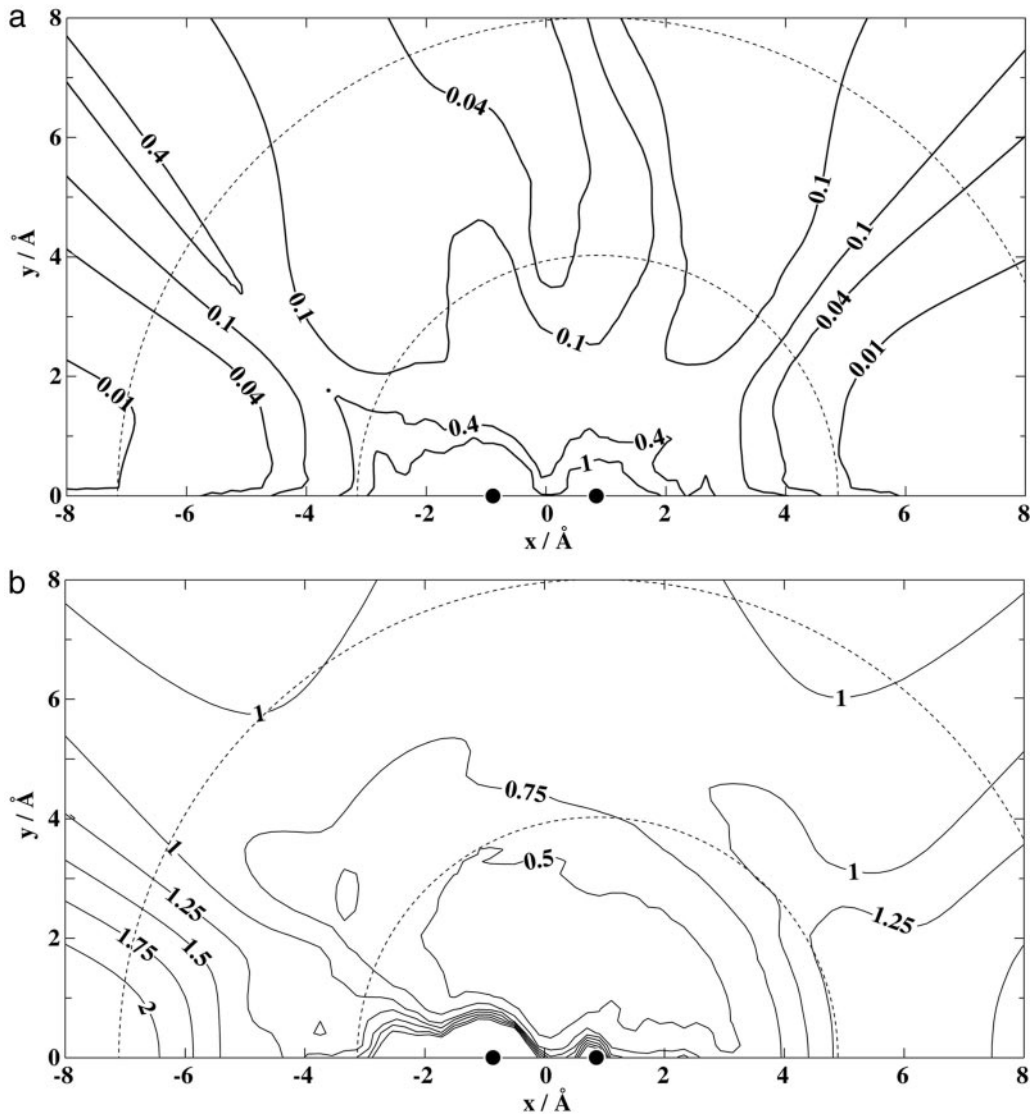

FIG. 9. Reliability of distance measurement in a three-spin system, relative to the two-spin case, in a powder sample using (a) the spin-diffusion and (b) the "weak coupling" Hamiltonians. The distance, r, is measured with respect to the fixed nucleus at (0.76, 0) Å.

$$\langle Q(t)\rangle = \sum_{r,s} Q^{\dagger}_{rs}\sigma_{sr}(0)\exp(i(\omega_r - \omega_s)t), \qquad [9]$$

where $\boldsymbol{Q}$ and $\boldsymbol{\sigma}(0)$ are the observable operator and the initial density matrix, respectively, and ω_r is the rth eigenvalue of the Hamiltonian, where r spans the Hilbert space of the operators. The term $Q^{\dagger}_{rs}\sigma_{sr}(0)$ is the amplitude of the transition r, s that has the frequency $\omega_r - \omega_s$. For simplicity we consider the special geometry of Fig. 10 where the spins form an isosceles triangle, that is, the remote spin is placed equidistantly from the two fixed spins such that the couplings of the remote spin to the fixed spins are identical. This symmetry allows the further block diagonalization of the Hamiltonian and reduces the number of "allowed" transitions. Note that it is possible to derive analytical expressions for the evolution in terms of the ratio of the couplings, since blocks of the symmetrized Hamiltonian are no bigger than 2×2. These formulas can be rather cumbersome, however, and Fig. 11a shows the result of numerical diagonalization of the Hamiltonian and the resulting "transition probabilities" as a function of the ratio between the nominally weak coupling and the coupling between the fixed spins. We are neglecting relaxation, and so this analysis is only directly applicable to situations where the coupling is larger than the effective linewidth.

When the recoupled Hamiltonian has the same form as the homonuclear dipolar interaction, Fig. 11a, there is a single nonzero transition frequency; the remaining component of the evolution has zero frequency, i.e., it is a constant offset. As the

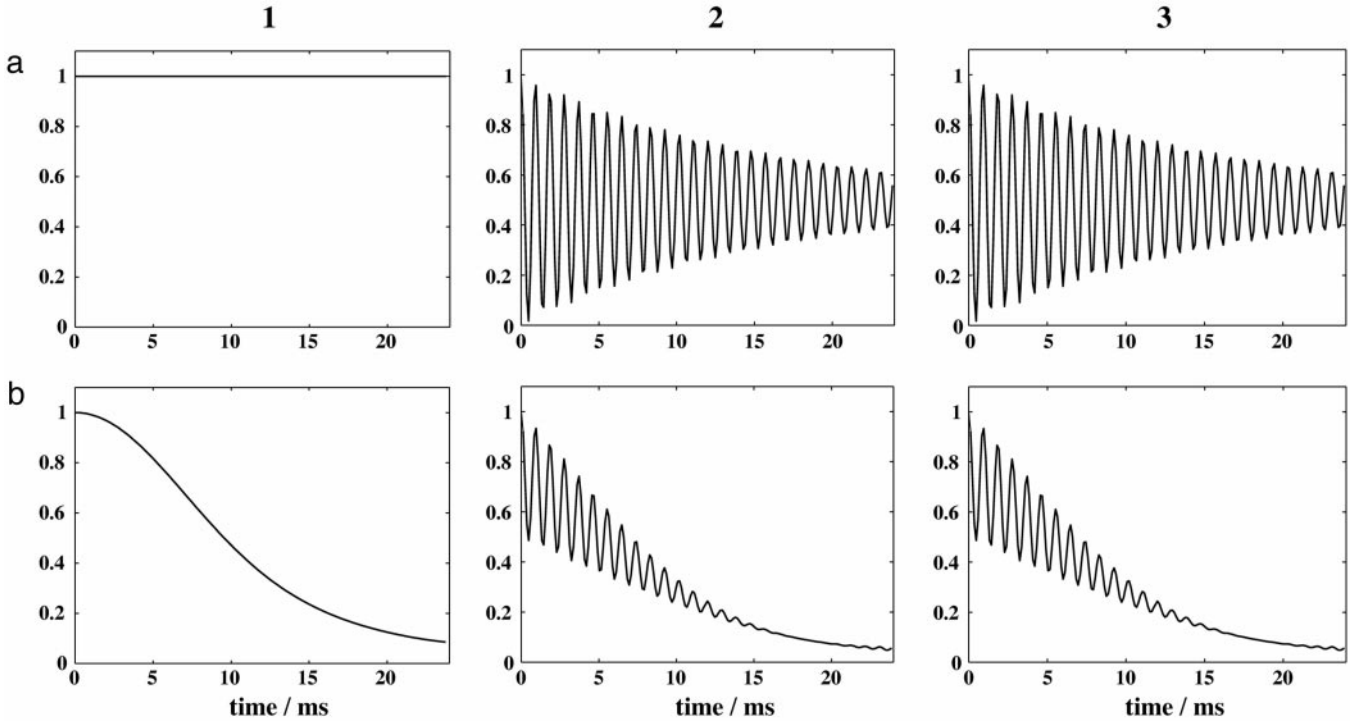

FIG. 10. Diagonal peak intensities for magnetization exchange in a three-spin system for a single orientation, $\Omega_{MR} = (\pi/2, \pi/2, 0)$, under (a) the spin diffusion and (b) the weak coupling Hamiltonians. The "probe" spin (leftmost panel) is placed symmetrically between the fixed spins at a distance of 5 Å.

distance to the remote spin increases, the transition frequency naturally tends toward that of the bonded pair. More significantly, its amplitude drops to zero. Since the fitting of the distance to the remote spin requires in effect the quantification of this coupling, the reliability of the distance measurement also falls rapidly. It is also worth noting that, since there is only one frequency present, any errors in the estimate of the strong coupling (which is assumed to be known) will strongly affect the quantification of the remote distance.

Unsurprisingly, this Fourier analysis of the time evolution is simpler for the weak coupling Hamiltonian, Fig. 11b. There is single oscillation of nonzero frequency present, whose frequency can be identified directly with the coupling between the remote and fixed spins (hence the linear slop of the log–log plot). Because all the terms of the Hamiltonian commute, the transition probability is constant. Hence, the reliability of the coupling measurement does not fall as rapidly with distance as is the case for noncommuting Hamiltonians.

It is worth noting that this "dipolar truncation" effect varies widely between different noncommuting Hamiltonians. Figure 11c, for example, shows the corresponding plots for recoupling using the C7 sequence (*7*), or its more broad-band variants (*25*). This Hamiltonian for the spin pair i, j has the form $H_{i,j} = cT^{i,j}_{2,2} + c^*T^{i,j}_{2,-2}$, where c is a scaling factor. Although the different terms of this Hamiltonian do not commute, $[H_{i,j}, H_{j,k}] \neq 0$, the suppression of the oscillatory components of the magnetization as the distance increases is less marked than for the spin-diffusion Hamiltonian of Fig. 11a. Calculations of distance reliabilities for powders show that the C7 double-quantum Hamiltonian indeed performs significantly better than the "spin diffusion" Hamiltonian, although not as well the weak coupling Hamiltonian, particularly at longer distances.

CONCLUSIONS

In this paper, we have considered the precision of distance measurements obtained from fitting the evolution of a dipolar-coupled spin system. For two-spin systems, the determination of distance information from exchange under the influence of the single dipolar coupling is straightforward. Leaving aside questions of differing systematic errors, the accuracy is maximized by using the Hamiltonian that recouples the dipolar interaction most strongly.

The more significant question addressed is whether it is feasible to determine geometrical information from systems of more than two dipolar-coupled spins. We have shown that the answer is strongly dependent on the nature of the coupling Hamiltonian. Using existing *homonuclear* recoupling Hamiltonians, and in particular those based on the normal homonuclear coupling Hamiltonian, it is clear that the complex interference between terms in a multispin system greatly reduces the precision of distance measurement. This is especially true at longer distances where weaker couplings are "truncated" by the presence of much stronger couplings. As the

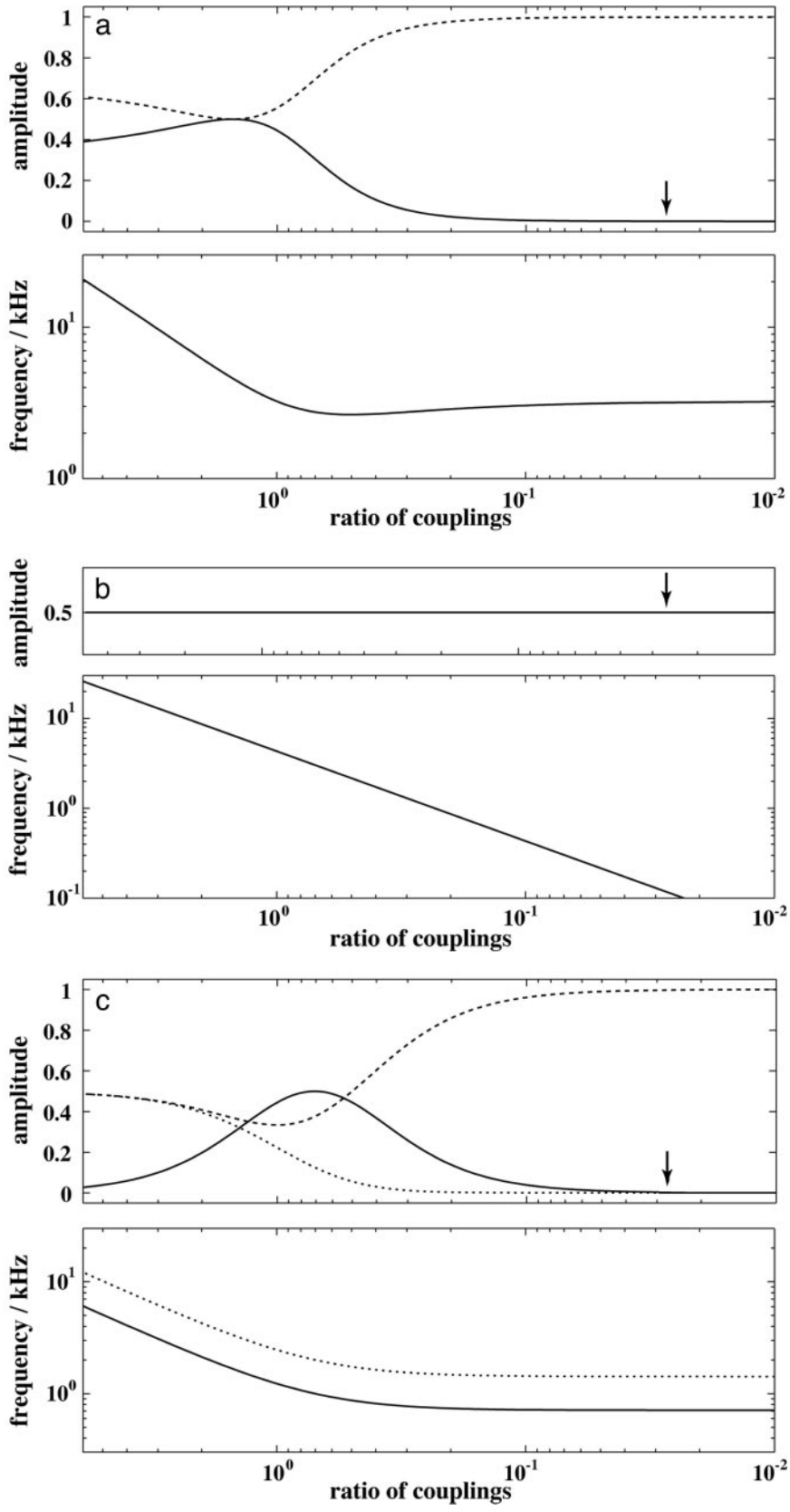
a
amplitude
1
0.8
0.6
0.4
0.2
0
frequency / kHz
10^1
10^0
10^0
10^{-1}
10^{-2}
ratio of couplings
b
amplitude
0.5
frequency / kHz
10^1
10^0
10^{-1}
10^0
10^{-1}
10^{-2}
ratio of couplings
c
amplitude
1
0.8
0.6
0.4
0.2
0
frequency / kHz
10^1
10^0
10^0
10^{-1}
10^{-2}
ratio of couplings

number of spins (and the number of free parameters) increases, the accuracy of the fitting can only diminish further. Thus, even assuming that the experimental exchange curves can be confidently fitted to simulations, it would seem that the *precise* measurement of distance information from the evolution of multispin systems is unlikely to be practical.

A notable exception occurs when the individual pair interactions of the Hamiltonian commute with each other, as is the case for *heteronuclear* recoupling in $I_N S$ systems if any homonuclear coupling between the I spins can be neglected. In this case, added couplings simply cause sequential splittings of the spectral features. As for J couplings in the weak-coupling limit in liquid-state NMR, the dipolar couplings in single crystal samples can then be accurately measured. Even in the powder, where the simplicity of the single orientation signals is obscured by the orientational dependence of the couplings, the accuracy of the results derived from three-spin simulations are very similar to those obtained from simple two-spin systems. This will also be true for larger spin systems. The simultaneous measurement of large and small dipolar couplings not only limits the need for selective labeling, but would allow the use of known internuclear distances to calibrate the experimental parameters, such as the recoupling pulse sequence scaling factor.

The ideal would obviously be to find a *homonuclear* recoupling Hamiltonian that satisfied the condition that pair coupling terms all commute with each other. As discussed in the appendix, it appears that this is unlikely with the conventional approach to creating average Hamiltonians using rotor-synchronized pulse sequences. While broadband homonuclear recoupling schemes are obviously appropriate for isolated spin pairs and for qualitative information on coupling strengths, they would seem to be of limited application for quantifying couplings in complex spin systems.

APPENDIX

In this appendix, we can consider whether it is possible to use rotor-synchronized pulse sequences to create a zero-order average Hamiltonian in which different pair coupling terms commute with each other.

Although recoupling Hamiltonians that contained multiple spin coupling terms, such as $I_{ix}I_{jy}I_{kx}$, may be of interest in their own right, we are here only concerned with Hamiltonians that retain the normal form of a pair coupling Hamiltonian. In other words, the coupling term for a given spin pair i, j contains only bilinear terms in i and j. Such a Hamiltonian can be written

$$H_{ij} = \vec{\boldsymbol{I}}_i \cdot \boldsymbol{A} \cdot \vec{\boldsymbol{I}}_j^{\mathrm{T}} \qquad [10]$$

where $\vec{\boldsymbol{I}}_i$ is the vector of spin operators, (I_{ix}, I_{iy}, I_{iz}). The matrix $\boldsymbol{A}$ describes the linear combination, A_{xx} being the coefficient of the $I_{ix}I_{jx}$ operator, etc. Hence, the heteronuclear Hamiltonian has $A_{zz} = 2$ as its only nonzero element, while the homonuclear coupling would be represented

$$A_{\mathrm{homo}} = \begin{pmatrix} -1 & 0 & 0 \\ 0 & -1 & 0 \\ 0 & 0 & 2 \end{pmatrix}. \qquad [11]$$

We now find the form of $\boldsymbol{A}$ such that all the coupling Hamiltonians commute. Terms that share no common spins must commute, $[H_{ij}, H_{kl}] = 0$, as must terms with themselves, $[H_{ij}, H_{ij}] = 0$. Hence, the condition that the coupling Hamiltonians mutually commute rests on the commutators of the form $[H_{ij}, H_{jk}]$. We can expand this commutator in terms of the matrix $\boldsymbol{A}$:

$$[H_{ij}, H_{jk}] = [\sum_{m,n} I_{im}A_{mn}I_{kn}, \sum_{m',n'} I_{jm'}A_{m'n'}I_{kn'}] \qquad [12]$$

$$= \sum_{m,n'} I_{im}I_{kn'} \sum_{m',n} A_{mn}A_{m'n'}[I_{jn}, I_{jm'}]. \qquad [13]$$

For this commutator to be identically zero, we require

$$\sum_{m',n} A_{mn}A_{m'n'}[I_{jn}, I_{jm'}] \equiv 0 \quad \forall\, m, n'. \qquad [14]$$

Using the properties of commutators, $[A, B] = -[B, A]$ and $[A, A] = 0$, we can write this as

$$\sum_{m'} \sum_{n>m'} A_{mn}A_{m'n'}[I_{jn}, I_{jm'}] + A_{mm'}A_{nn'}[I_{jm'}, I_{jn}] \qquad [15]$$

$$= \sum_{m'} \sum_{n>m'} (A_{mn}A_{m'n'} - A_{mm'}A_{nn'})[I_{jn}, I_{jm'}] \equiv 0 \quad \forall\, m, n'. \qquad [16]$$

Since the sums over m' and n run uniquely over the nonzero commutator pairings $xy \rightarrow z$, $xz \rightarrow -y$, and $yz \rightarrow x$, the condition that the Hamiltonian pairs commute with each other is reduced to

FIG. 11. Amplitude and frequency of the oscillations present in the evolution of the magnetization of the remote spin in the three-spin system for a single orientation using (a) a spin diffusion Hamiltonian, (b) the "weak coupling" Hamiltonian, (c) the C7 Hamiltonian. The amplitude and frequency for each transition are drawn with the same line type, with a longer dashed line being used for the amplitude of any zero-frequency component. The remote spin is placed symmetrically between the fixed spins and the x coordinate is the ratio between the coupling to the remote spin and the coupling between the fixed nuclei. The arrow marks the geometry of Fig. 10.

$$A_{mn}A_{m'n'} \equiv A_{mm'}A_{nn'} \quad \forall\, m,\, n',\, m',\, n \text{ with } n > m'. \qquad [17]$$

The general solution to this equation is $A_{mn} = \alpha_m\alpha_n$, i.e.,

$$A \equiv \begin{pmatrix} \alpha_x\alpha_x & \alpha_x\alpha_y & \alpha_x\alpha_z \\ \alpha_x\alpha_y & \alpha_y\alpha_y & \alpha_y\alpha_z \\ \alpha_x\alpha_z & \alpha_y\alpha_z & \alpha_z\alpha_z \end{pmatrix}. \qquad [18]$$

A is then uniquely specified by three parameters, α_x, α_y, and α_z. This condition is clearly true for the heteronuclear coupling Hamiltonian and false for the homonuclear coupling.

The next question is whether coupling matrices of this form can be generated starting from the homonuclear coupling Hamiltonian. The conventional approach to such a problem is to find a cyclic rotor-synchronized pulse sequence that creates an average Hamiltonian with the required properties, at least to zero order. This average Hamiltonian is determined via an interaction or toggling frame that is rotated by the pulses. Provided the RF is synchronized with the rotor and is cyclic (in the sense that the interaction returns to its original orientation at the start of each rotor cycle), then the effective Hamiltonian is given to zero order by the average of the interaction frame Hamiltonian (*26*).

In terms of irreducible spherical tensor operators, the homonuclear coupling at high field is proportional to $T_{2,0}$. In its interaction frame representation at an arbitrary point in the rotor cycle, this Hamiltonian will thus be $T_{2,0}$ rotated through a time- and sequence-dependent set of Euler angles. Since rotations simply transform the operators of a given rank (here 2) among themselves, the final zero-order average Hamiltonian must be a linear combination of $T_{2,m}$ operators (*7*, *27*)

$$\bar{H}^{(0)} = \sum_{m=-2}^{2} c_m T_{2,m} \quad c_m = (-1)^m c^*_{-m}. \qquad [19]$$

The elements of the $\boldsymbol{A}$ matrix (Cartesian representation) can be expressed in terms of the c_m coefficients for the spherical tensor representation. Unfortunately it soon becomes apparent that no combination of c_m values can satisfy Eq. [18]. Because $\boldsymbol{A}$ must be decomposed solely in terms of rank 2 components, it must be traceless; hence, $\alpha_z^2 = -\alpha_x^2 - \alpha_y^2$. This means that α_z must be imaginary if α_x and α_y are taken to be real, leading to imaginary off-diagonal elements of $\boldsymbol{A}$ (A_{xz} and A_{yz}). It is impossible to generate a purely real matrix of the form of Eq. [18] that is also traceless. Imaginary components of $\boldsymbol{A}$ cannot be generated by rotation from $T_{2,0}$ without breaking the conjugation symmetry of the c_m and c_{-m} terms. The self-commuting Hamiltonian requires in effect the creation of an "isotropic" mixing Hamiltonian $I_{ix}I_{jx} + I_{iy}I_{jy} + I_{iz}I_{jz}$. Note that $\boldsymbol{A}$ corresponding to the heteronuclear coupling Hamiltonian, $2I_{iz}I_{jz}$, has a nonzero trace and so cannot be decomposed into purely rank 2 terms. It thus appears that *cyclic* rotor-synchronized pulse sequences cannot be used to create an average Hamiltonian with the desired properties.

ACKNOWLEDGMENTS

P.H. was supported during this work by a Marie Curie fellowship from the European Commission (contract number ERBFMBICT961185). We are grateful to Anja Böckmann and Stefano Caldarelli for interesting discussions. The parallel computations were carried out using the facilities of the Pôle Scientifique de Modelisation Numerique in Lyon.

REFERENCES

1. A. E. Bennett, R. G. Griffin, and S. Vega, Recoupling of homo- and heteronuclear dipolar interactions in rotating solids, *NMR Basic Principles and Progress* **33,** 1–77 (1994).
2. T. G. Oas, R. G. Griffin, and M. H. Levitt, Rotary resonance recoupling of dipolar interactions in solid-state nuclear magnetic resonance spectroscopy, *J. Chem. Phys.* **89,** 692–695 (1988).
3. M. H. Levitt, D. P. Raleigh, F. Creuzet, and R. G. Griffin, Theory and simulations of homonuclear spin pair systems in rotating solids, *J. Chem. Phys.* **92,** 6347–6364 (1990).
4. A. E. Bennett, J. H. Ok, and R. G. Griffin, Chemical shift correlation spectroscopy in rotating solids: Radio frequency-driven dipolar recoupling and longitudinal exchange, *J. Chem. Phys.* **96,** 8624–8627 (1992).
5. M. Baldus, M. Tomaselli, B. H. Meier, and R. R. Ernst, Broadband polarization-transfer experiments for rotating solids, *Chem. Phys. Lett.* **230,** 329–336 (1994).
6. B.-Q. Sun, P. R. Costa, D. Kocisko, J. P. T. Lansbury, and R. G. Griffin, Internuclear distance measurements in solid state nuclear magnetic resonance: Dipolar recoupling via rotor synchronized spin locking, *J. Chem. Phys.* **102,** 702–707 (1995).
7. Y. K. Lee, N. D. Kurur, M. Helme, O. G. Johannessen, N. C. Nielsen, and M. H. Levitt, Efficient dipolar recoupling in the NMR of rotating solids. A sevenfold symmetric radiofrequency pulse sequence, *Chem. Phys. Lett.* **242,** 304–309 (1995).
8. S. Kühne, M. A. Mehta, J. A. Stringer, D. M. Gregory, J. C. Shiels, and G. P. Drobny, Distance measurements by dipolar recoupling two-dimensional solid-state NMR, *J. Phys. Chem. A* **102,** 2274–2282 (1998).
9. A. E. Bennett, C. M. Rienstra, and J. M. Griffiths, Homonuclear radio frequency-driven recoupling in rotating solids, *J. Chem. Phys.* **108,** 9463–9479 (1998).
10. P. Robyr, B. H. Meier, and R. R. Ernst, Radio-frequency-driven nuclear spin diffusion in solids, *Chem. Phys. Lett.* **162,** 417–423 (1989).
11. A. van den Bos, Parameter estimation, in "Handbook of Measurement Science" (P. H. Sydenham, Ed.), Wiley, New York (1982).
12. J. P. Norton, "An Introduction to Identification," Academic Press, New York (1986).
13. W. H. Press, S. A. Teukolsky, W. T. Vetterling, and B. P. Flannery, "Numerical Recipes in C," 2nd ed., Cambridge Univ. Press, Cambridge (1992).
14. S. Parkin, B. Rupp, and H. Hope, Structure of bovine pancreatic trypsin inhibitor at 125K: definition of carboxyl-terminal residues Gly57 and Ala58, *Acta Crystallogr.* **D52,** 18–29 (1996).
15. P. Hodgkinson and P. J. Hore, Sampling and the quantification of NMR data, *Adv. Magn. Opt. Reson.* **20,** 187–244 (1997).

16. M. Ernst, A. C. Kolbert, K. Schmidt-Rohr, and A. Pines, Isotropic second-order dipolar shifts in the rotating frame, *J. Chem. Phys.* **104,** 8258–8268 (1996).

17. M. Ernst, S. Bush, A. C. Kolbert, and A. Pines, Second-order recoupling of chemical-shielding and dipolar-coupling tensors under spin decoupling in solid-state NMR, *J. Chem. Phys.* **105,** 3387–3397 (1996).

18. T. Gullion and J. Schaefer, Rotational-echo double-resonance NMR, *J. Magn. Reson.* **81,** 196–200 (1989).

19. T. Gullion and J. Schaefer, Detection of weak heteronuclear dipolar coupling by rotational-echo double-resonance nuclear magnetic resonance, *Adv. Magn. Reson.* **13,** 57–83 (1989).

20. N. Tjandra and A. Bax, Direct measurement of distances and angles in biomolecules by NMR in a dilute liquid crystalline medium, *Science* **278,** 1111–1114 (1997).

21. J. M. Goetz and J. Schaefer, REDOR dephasing by multiple spins in the presence of molecular motion, *J. Magn. Reson.* **127,** 147–154 (1997).

22. T. Gullion and C. H. Pennington, θ-REDOR: an MAS NMR method to simplify multiple coupled heteronuclear spin systems, *Chem. Phys. Lett.* **290,** 88–93 (1998).

23. G. McGeorge, R. K. Harris, A. V. Churakov, A. M. Chippendale, J. F. Bullock, and Z. Can, Analysis of a solid state conformational rearrangement using ^{15}N NMR and X-ray crystallography, *J. Phys. Chem. A* **102,** 3505–3513 (1998).

24. P. Hodgkinson and L. Emsley, The reliability of the determination of tensor parameters by solid-state nuclear magnetic resonance, *J. Chem. Phys.* **107,** 4808–4816 (1997).

25. M. Hohwy, H. J. Jakobsen, M. Edén, M. H. Levitt, and N. C. Nielsen, Broadband dipolar recoupling in the nuclear magnetic resonance of rotating solids: A compensated C7 pulse sequence, *J. Chem. Phys.* **108,** 2686–2694 (1998).

26. U. Haerberlen, High resolution NMR spectroscopy in solids, *Adv. Magn. Reson.* **Suppl. 1** (1976).

27. R. Tycko, Zero field magnetic resonance in high field, *J. Chem. Phys.* **92,** 5776–5793 (1990).